

A Ribosome-Bound Quality Control Complex Triggers Degradation of Nascent Peptides and Signals Translation Stress

Onn Brandman,^{1,2,4} Jacob Stewart-Ornstein,^{1,2,4} Daisy Wong,^{1,2,4} Adam Larson,³ Christopher C. Williams,^{1,2,4} Gene-Wei Li,^{1,2,4} Sharleen Zhou,⁵ David King,⁵ Peter S. Shen,⁶ Jimena Weibezahn,^{1,2,4} Joshua G. Dunn,^{1,2,4} Silvi Rouskin,^{1,2,4} Toshifumi Inada,⁷ Adam Frost,^{6,*} and Jonathan S. Weissman^{1,2,4,*}

¹Department of Cellular and Molecular Pharmacology

²California Institute for Quantitative Biomedical Research

³Department of Biochemistry and Biophysics

⁴Howard Hughes Medical Institute

University of California, San Francisco, San Francisco, CA 94158, USA

⁵HHMI Mass Spectrometry Laboratory, University of California, Berkeley, Berkeley, CA 94720, USA

⁶Department of Biochemistry and Huntsman Cancer Institute, University of Utah School of Medicine, Salt Lake City, UT 84112, USA

⁷Graduate School of Pharmaceutical Science, Tohoku University, Sendai 980-8578, Japan

*Correspondence: frost@biochem.utah.edu (A.F.), weissman@cmp.ucsf.edu (J.S.W.)

<http://dx.doi.org/10.1016/j.cell.2012.10.044>

SUMMARY

The conserved transcriptional regulator heat shock factor 1 (Hsf1) is a key sensor of proteotoxic and other stress in the eukaryotic cytosol. We surveyed Hsf1 activity in a genome-wide loss-of-function library in *Saccharomyces cerevisiae* as well as ~78,000 double mutants and found Hsf1 activity to be modulated by highly diverse stresses. These included disruption of a ribosome-bound complex we named the Ribosome Quality Control Complex (RQC) comprising the Ltn1 E3 ubiquitin ligase, two highly conserved but poorly characterized proteins (Tae2 and Rqc1), and Cdc48 and its cofactors. Electron microscopy and biochemical analyses revealed that the RQC forms a stable complex with 60S ribosomal subunits containing stalled polypeptides and triggers their degradation. A negative feedback loop regulates the RQC, and Hsf1 senses an RQC-mediated translation-stress signal distinctly from other stresses. Our work reveals the range of stresses Hsf1 monitors and elucidates a conserved cotranslational protein quality control mechanism.

ACKNOWLEDGMENTS

We thank the members of the Weissman lab, M. Bassik, E. Boydston, L. Gilbert, A. Grenninger, C. Jan, M. Jonikas, M. Kampmann, Y. Liu, W. Luddington, M. McKeon, E. Oh, C. Reiger, M. Smith, N. Stern-Ginossar, and P. Walter for their valuable help with the manuscript and input on the

project; T. Becker and R. Beckmann for help with EM; M. Larson and B. Toyama for help with graphic design; and M. Szeto for help in creating the fluorescent reporters. O.B. was supported by a Helen Hay Whitney postdoctoral fellowship. This work was funded by the Howard Hughes Medical Institute (to J.S.W.).

Received: July 24, 2012

Revised: October 3, 2012

Accepted: October 30, 2012

Published: November 20, 2012

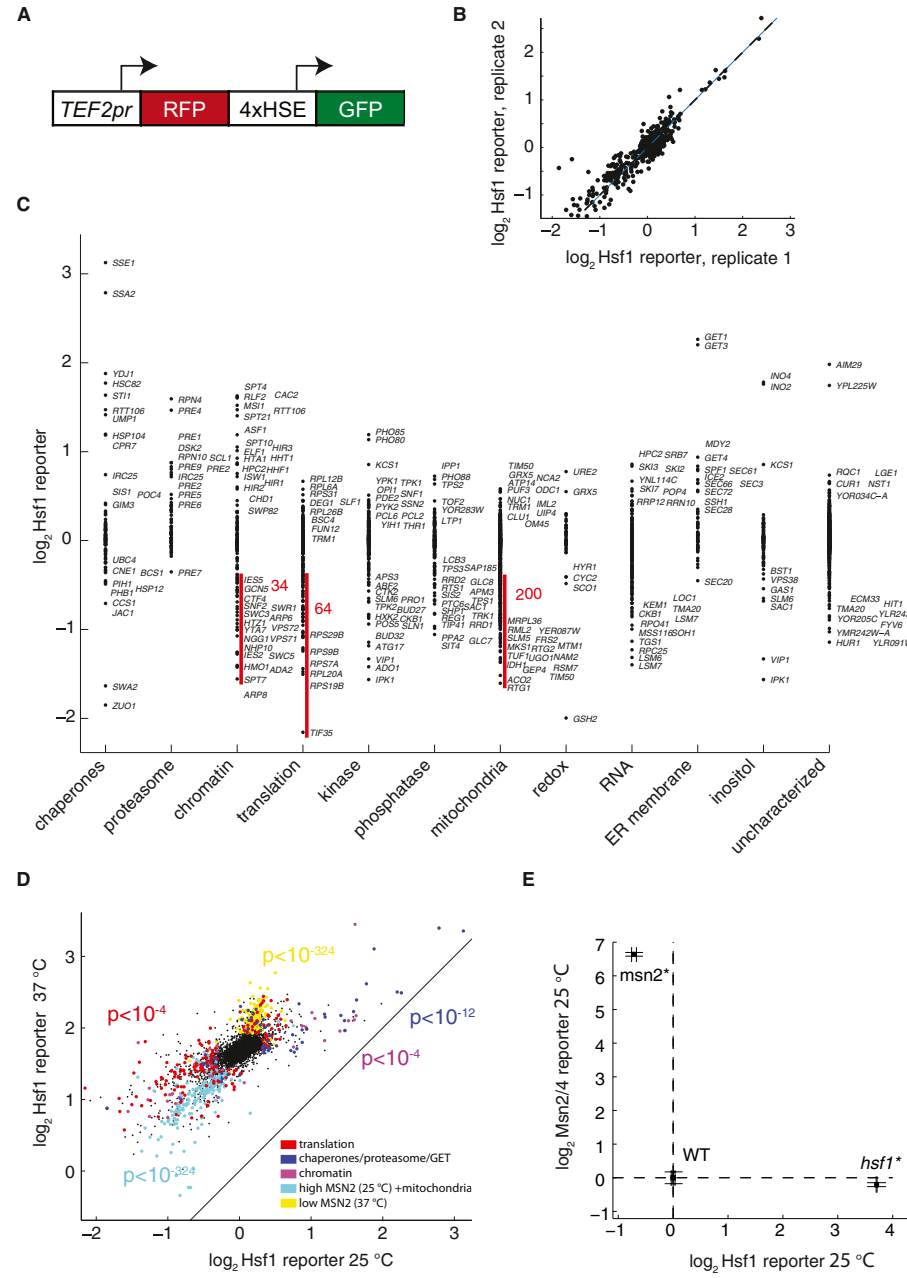
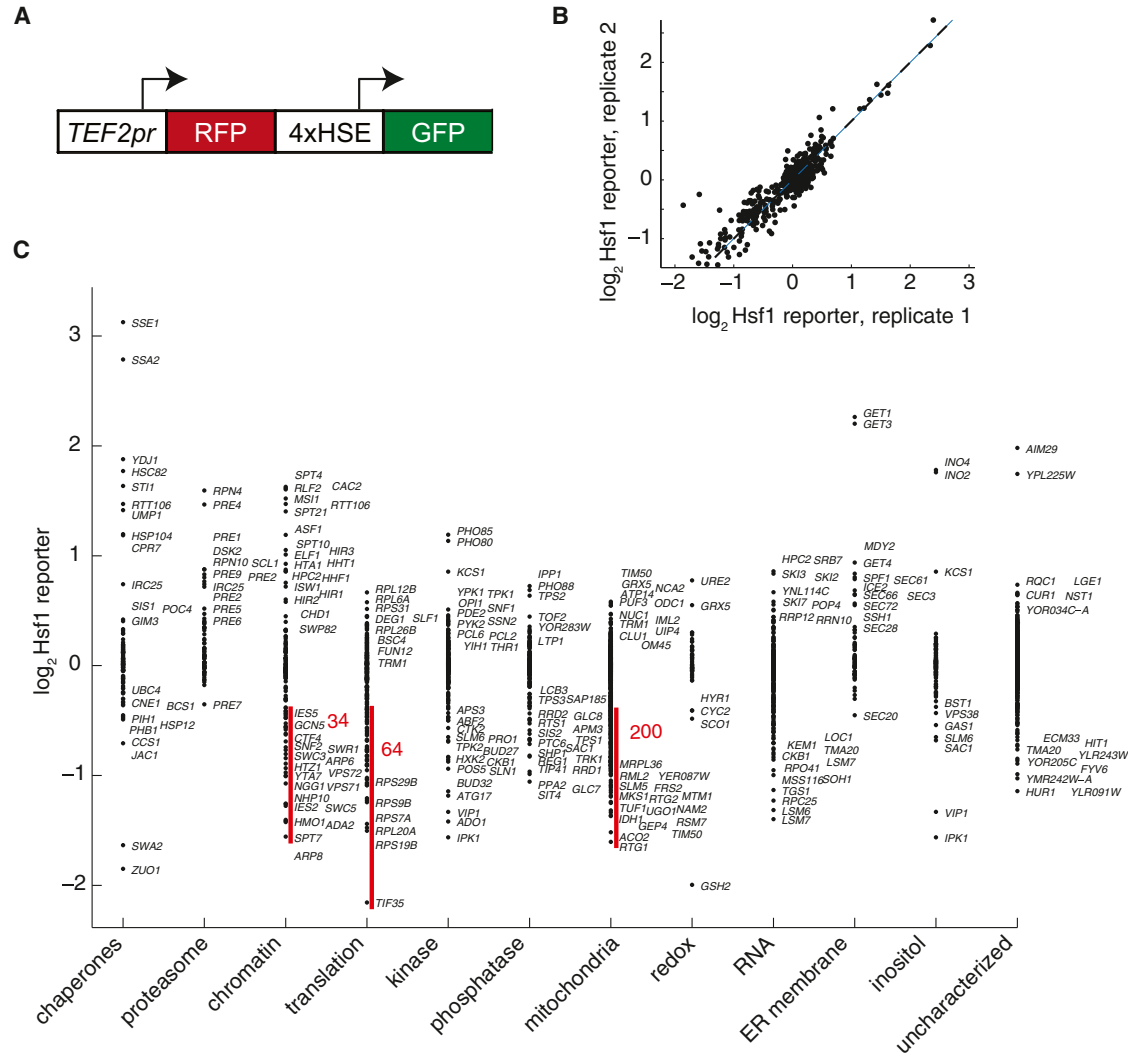


Figure 1. A Genome-wide Screen Reveals that Hsf1 Senses Diverse Stress Conditions

(A) Schematic diagram for fluorescent Hsf1 reporter. An RFP driven by the *TEF2* promoter and a GFP driven by a synthetic promoter with multiple Hsf1 binding sites were integrated in the *URA3* locus of the yeast genome.



(B) Independent crosses of reporter strain into 731 loss-of-function alleles (selected hits from full-genome screen) show allelic variation and reproducibility of the reporter system.

(C) Selected categories of annotated functions from genome-wide screen. Red bars indicate number of strains below an SD for selected categories. Genes beyond 1 SD are labeled as space is available, with full results in [Table S1](#).

(D) Hsf1 and Msn2/4 activities with genome-wide library of alleles at steady state (25°C) and after 1 hr heat shock at 37°C. p values from student's t test show enrichment for selected categories in each quadrant (delimited by 1 SD from the median).

(E) Effects of constitutively active *hsf1* allele (*hsf1**) and *msn2* allele (*msn2**) on Hsf1 and Msn2/4 activities at 25°C.

See also [Tables S1](#) and [S2](#) and [Figure S2](#).

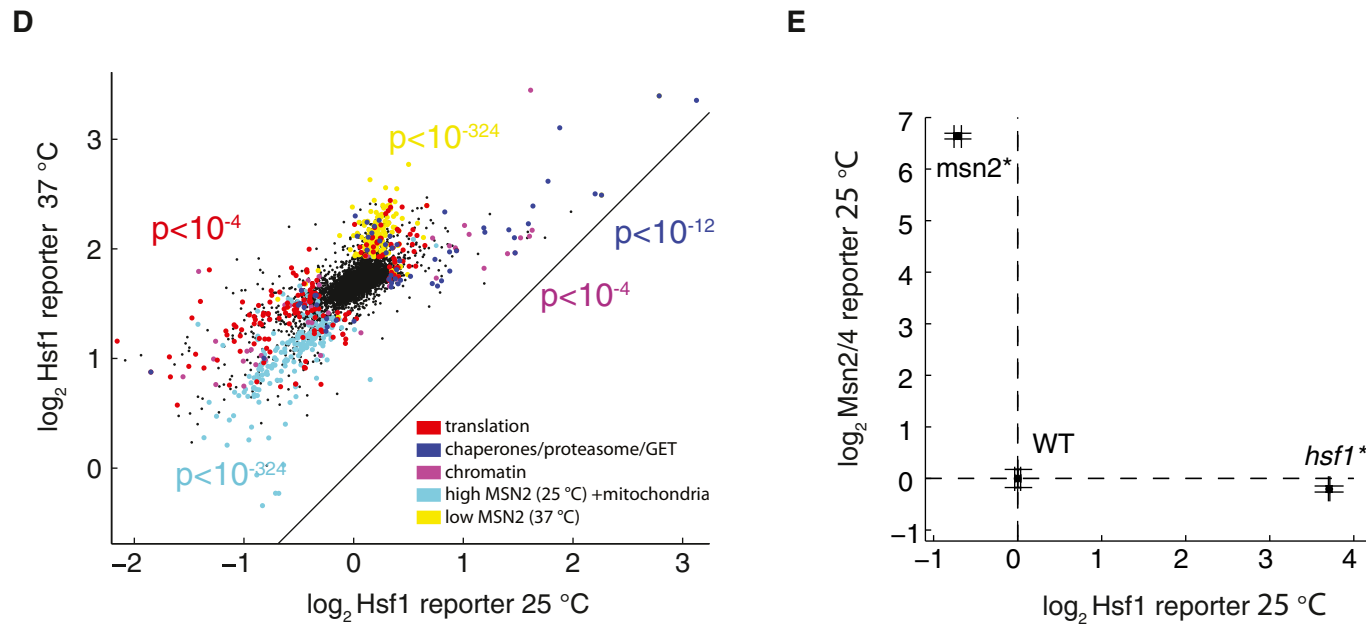


Figure 1. A Genome-wide Screen Reveals that Hsf1 Senses Diverse Stress Conditions

(A) Schematic diagram for fluorescent Hsf1 reporter. An RFP driven by the *TEF2* promoter and a GFP driven by a synthetic promoter with multiple Hsf1 binding sites were integrated in the *URA3* locus of the yeast genome.

(B) Independent crosses of reporter strain into 731 loss-of-function alleles (selected hits from full-genome screen) show allelic variation and reproducibility of the reporter system.

(C) Selected categories of annotated functions from genome-wide screen. Red bars indicate number of strains below an SD for selected categories. Genes beyond 1 SD are labeled as space is available, with full results in [Table S1](#).

(D) Hsf1 and Msn2/4 activities with genome-wide library of alleles at steady state (25°C) and after 1 hr heat shock at 37°C. p values from student's t test show enrichment for selected categories in each quadrant (delimited by 1 SD from the median).

(E) Effects of constitutively active *hsf1* allele (*hsf1**) and *msn2* allele (*msn2**) on Hsf1 and Msn2/4 activities at 25°C.

See also [Tables S1](#) and [S2](#) and [Figure S2](#).

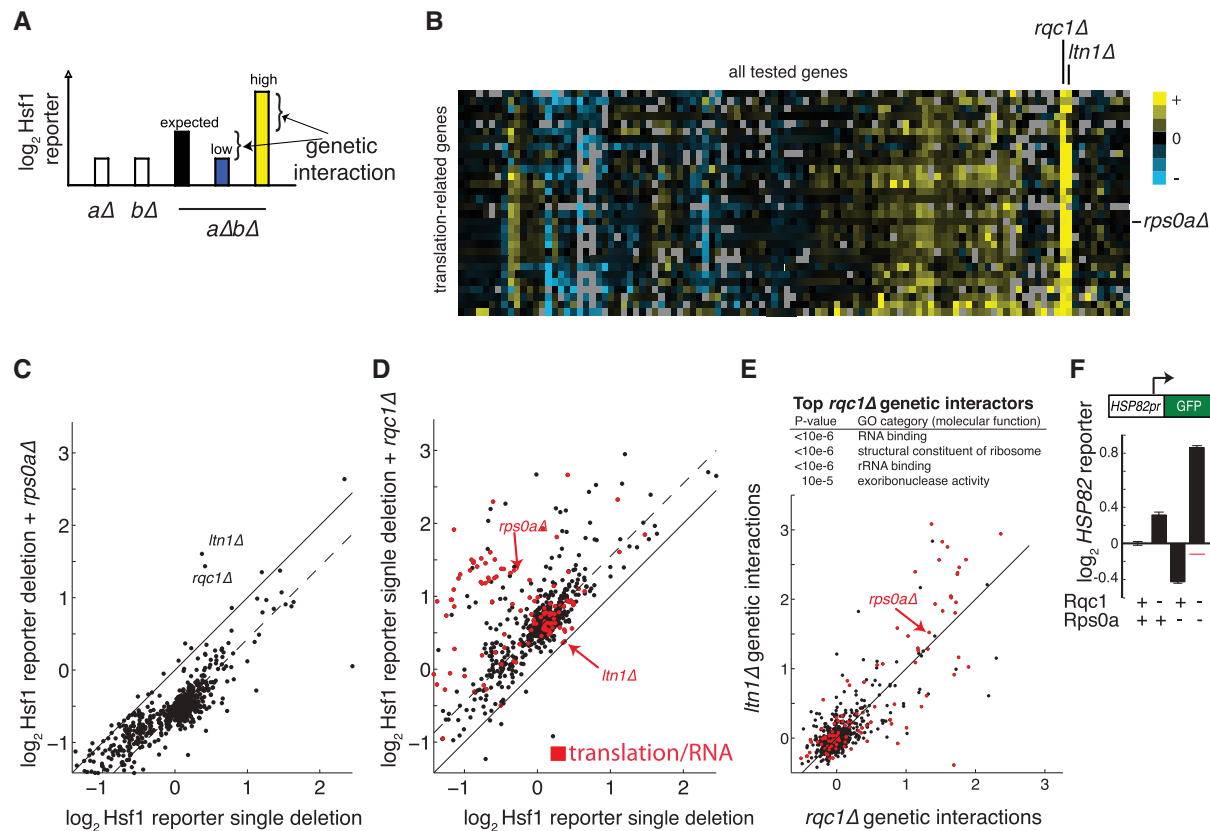


Figure 2. Translation Stress Identifies Ltn1 and Rqc1

(A) Schematic diagram illustrating the strategy for quantifying genetic interactions in double-mutant strains. An expected value for the double mutant is first computed based on single mutant reporter levels. The expected value is then compared to the actual double-mutant value to arrive at a genetic interaction score. Positive genetic interactions (double mutant is higher than expected) are colored in yellow, whereas negative genetic interactions (double mutant is lower than expected) are colored in blue.

(B) Genetic interactions corresponding to a set of translation-related genes that clustered together in a genetic interaction map.

(C and D) Hsf1 activity levels in single and double-mutant strains. The y axis of each graph shows double-mutant values for a common mutant ($rps0a\Delta$ or $rqc1\Delta$) combined with diverse alleles. Single mutant values appear on the x axis.

(E) Comparison of $ltn1\Delta$ and $rqc1\Delta$ genetic interaction scores. Inset: top enriched Gene Ontology (GO) categories of positive interactors with $rqc1\Delta$ from full-genome screen (see Tables S1 and S3).

(F) *HSP82* reporter levels showing a positive genetic interaction between $rqc1\Delta$ and $rps0a\Delta$ (red line denotes expected value of double mutant). Translation and RNA-related genes are marked in red in (D) and (E).

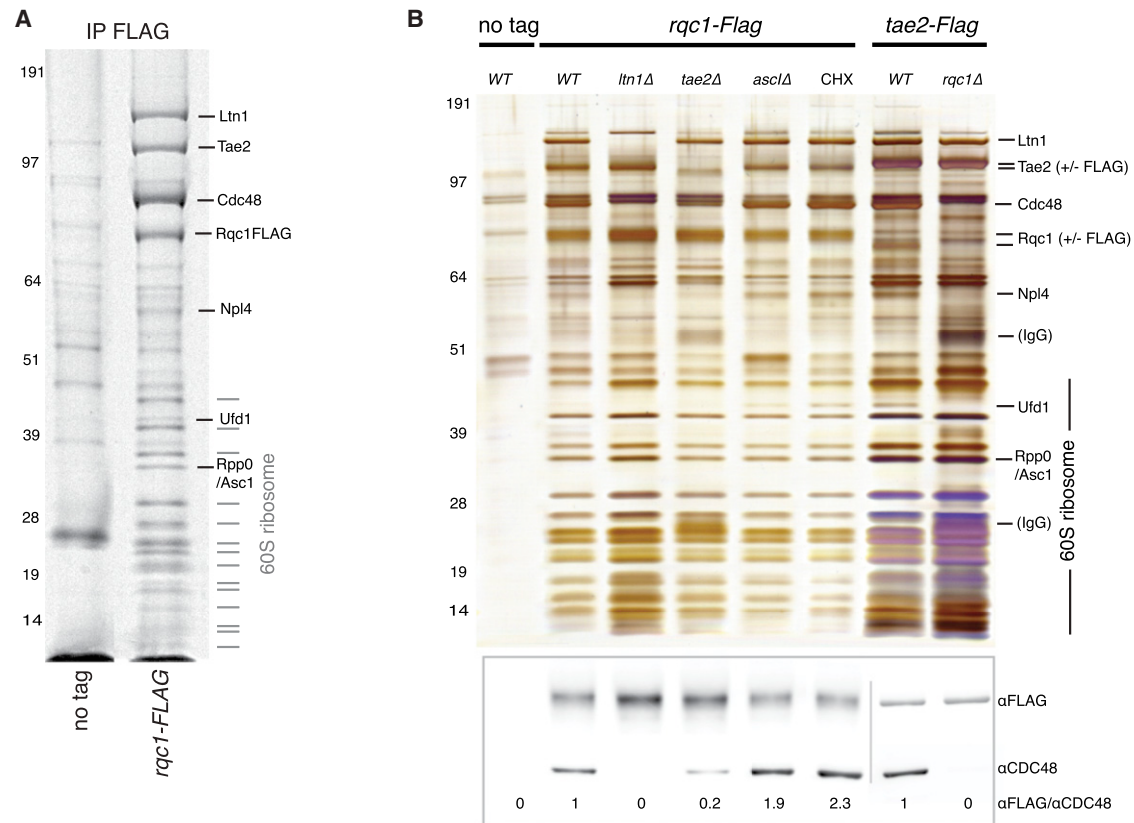


Figure 3. Rqc1/Ltn1 Organize a Larger Cotranslational Quality Control Complex

(A) IP of endogenously expressed Rqc1 3xFLAG fusion protein viewed with Coomassie staining. Selected nonbackground bands identified by mass spectrometry are labeled (all identified nonbackground bands available in [Figure S3](#)).

(B) Silver staining of Rqc1 and Tae2 IPs in selected deletion backgrounds and with cycloheximide (CHX) (100 μ g/ml, added 2 min before harvesting). Below, western blot for Cdc48 in IPs along with quantified amounts of Cdc48 (Cdc48/FLAG).

(C) RNA absorbance (260 nm) of 10%–50% sucrose gradient for input and output of Rqc1 IP. Each trace is independently scaled.

(D) Class averages of particles selected from electron micrographs of negatively stained *Rqc1-FLAG* IP in WT, *tae2Δ*, and *ltn1Δ* strain backgrounds.

(E) Western blot of a cotranslationally degraded model substrate containing a polybasic region expressed in RQC deletion strains.

(F) GFP levels in samples from (E) measured by using a flow cytometer and normalized to control.

(G) Western blot for monoubiquitin in IP samples.

See also [Figures S3](#), [S4](#), and [S5](#).

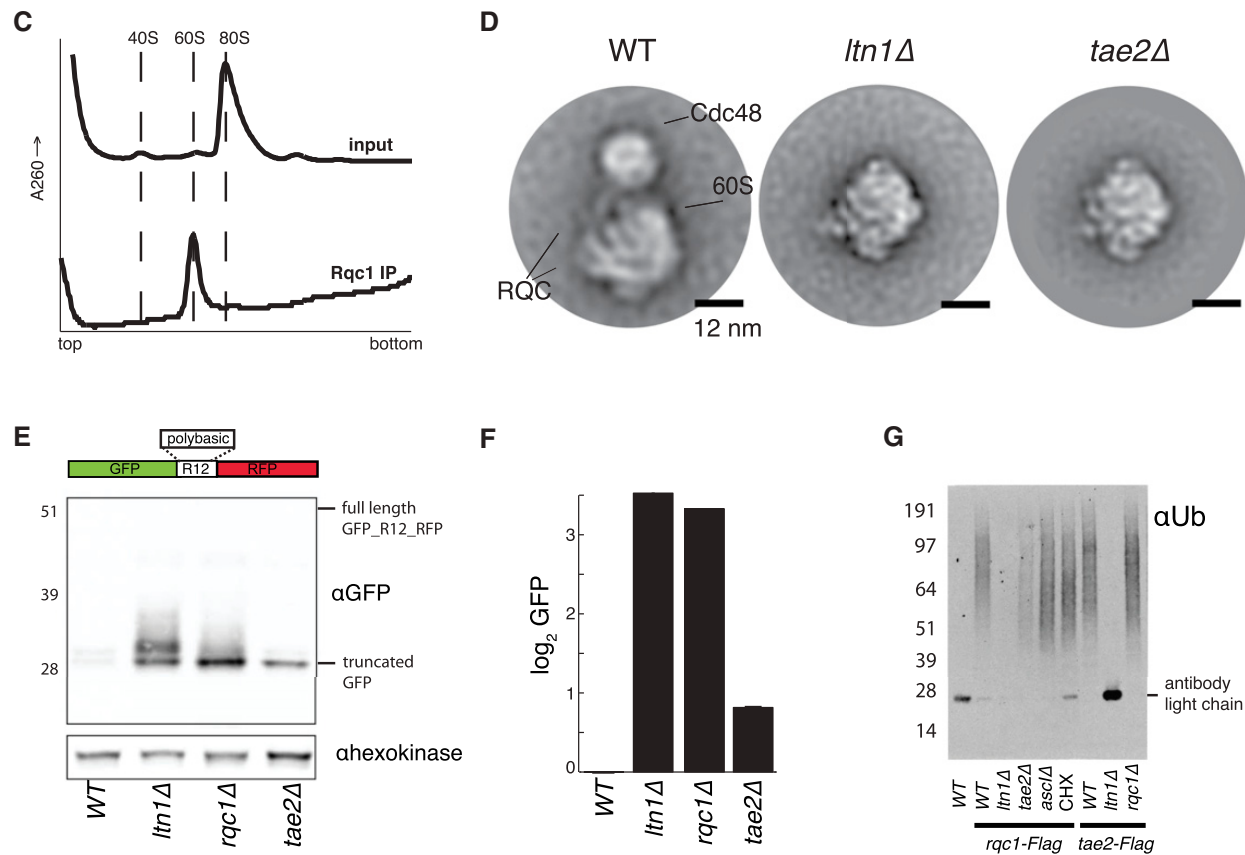


Figure 3. Rqc1/Ltn1 Organize a Larger Cotranslational Quality Control Complex

(A) IP of endogenously expressed Rqc1 3xFLAG fusion protein viewed with Coomassie staining. Selected nonbackground bands identified by mass spectrometry are labeled (all identified nonbackground bands available in [Figure S3](#)).

(B) Silver staining of Rqc1 and Tae2 IPs in selected deletion backgrounds and with cycloheximide (CHX) (100 μ g/ml, added 2 min before harvesting). Below, western blot for Cdc48 in IPs along with quantified amounts of Cdc48 (Cdc48/FLAG).

(C) RNA absorbance (260 nm) of 10%–50% sucrose gradient for input and output of Rqc1 IP. Each trace is independently scaled.

(D) Class averages of particles selected from electron micrographs of negatively stained Rqc1-FLAG IP in WT, tae2 Δ , and ltn1 Δ strain backgrounds.

(E) Western blot of a cotranslationally degraded model substrate containing a polybasic region expressed in RQC deletion strains.

(F) GFP levels in samples from (E) measured by using a flow cytometer and normalized to control.

(G) Western blot for monoubiquitin in IP samples.

See also [Figures S3, S4, and S5](#).

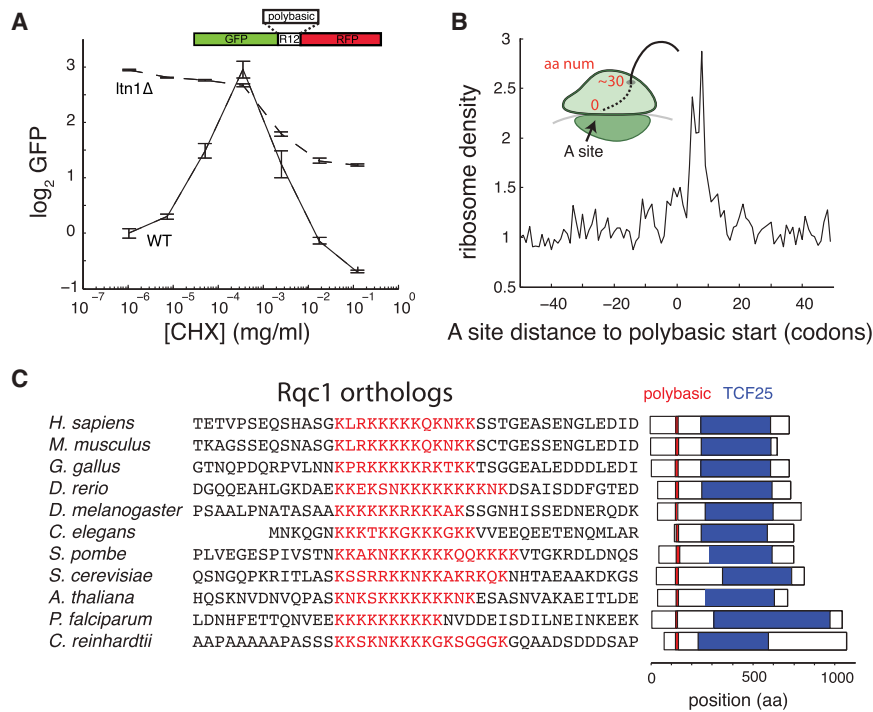


Figure 4. Rqc1 Levels Are Autoregulated by a Conserved Negative Feedback Loop

(A) GFP levels in strains expressing a contrtranslationally degraded polybasic reporter subject to 10 hr cycloheximide treatment at the indicated concentration.

(B) Ribosome footprint density at endogenous polybasic stretches (6 or greater K or R per 10 residues, n = 103).

(C) Conservation of Rqc1, with polybasic and TCF25 (Bateman et al., 2004) domains highlighted.

(D) Assay showing the ability of Rqc1 alleles (WT, *rqc1*-FLAG, *rqc1^{ala}*-FLAG, and *rqc1*Δ) to act upon a model cotranslationally degraded substrate.

(E) *rqc1*-FLAG and *rqc1^{ala}*-FLAG protein levels in deletion strains.

(F) Results of screen for regulators of a polybasic substrate (full results in Table S1). *tae2*Δ and the four strongest hits labeled.

(G) GFP and RFP levels of a polybasic substrate in selected hits from full-genome screen.

Also see Table S4 and Figure S6.

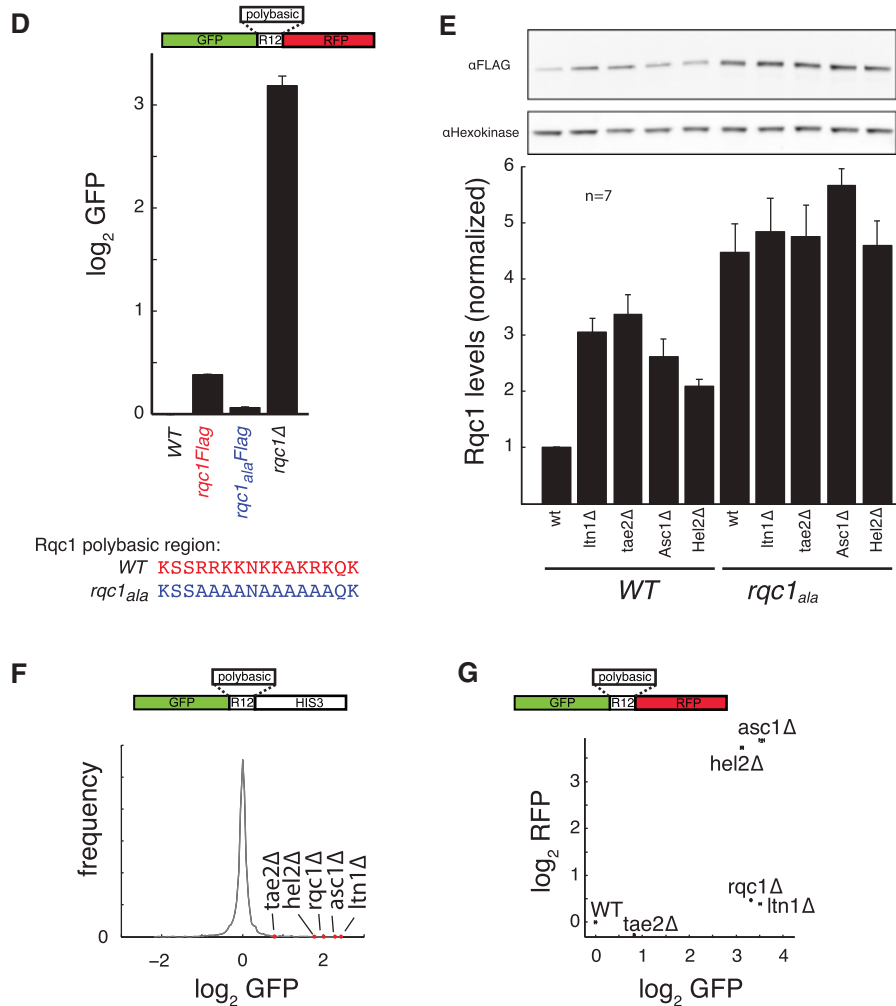


Figure 4. Rqc1 Levels Are Autoregulated by a Conserved Negative Feedback Loop

(A) GFP levels in strains expressing a contras translationally degraded polybasic reporter subject to 10 hr cycloheximide treatment at the indicated concentration.

(B) Ribosome footprint density at endogenous polybasic stretches (6 or greater K or R per 10 residues, $n = 103$).

(C) Conservation of Rqc1, with polybasic and TCF25 (Bateman et al., 2004) domains highlighted.

(D) Assay showing the ability of Rqc1 alleles (WT, *rqc1-FLAG*, *rqc1_{ala}-FLAG*, and *rqc1Δ*) to act upon a model cotranslationally degraded substrate.

(E) *rqc1-FLAG* and *rqc1_{ala}-FLAG* protein levels in deletion strains.

(F) Results of screen for regulators of a polybasic substrate (full results in Table S1). *tae2Δ* and the four strongest hits labeled.

(G) GFP and RFP levels of a polybasic substrate in selected hits from full-genome screen.

Also see Table S4 and Figure S6.

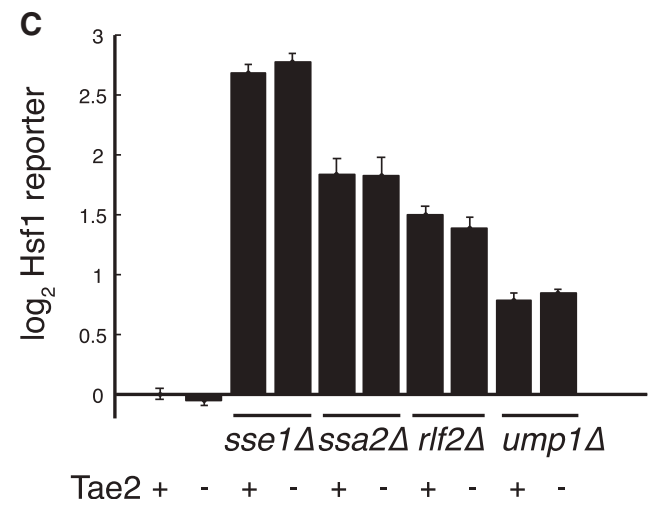
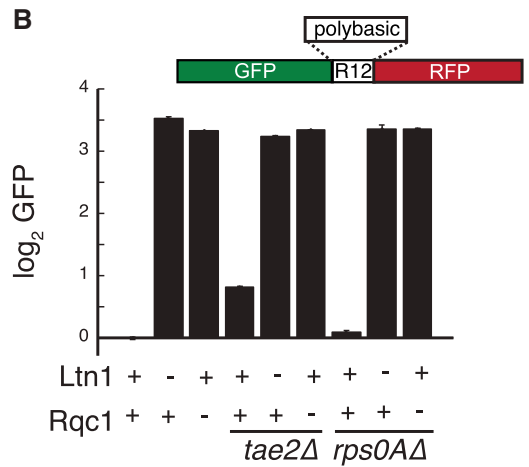
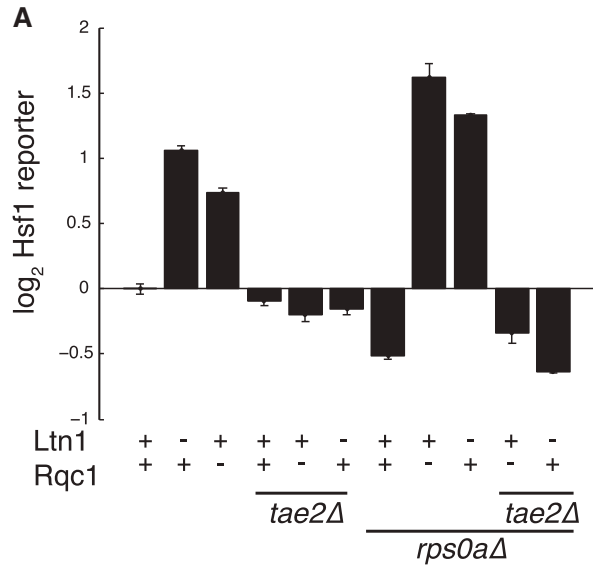


Figure 5. Tae2 Is Responsible for a Distinct Hsf1 Branch that Monitors Translation Stress

(A) Hsf1 activity in deletion strains for the RQC and a ribosomal subunit causing synergistic activation of Hsf1.
 (B) GFP levels of the cotranslationally degraded reporter construct in selected strain backgrounds from (A).
 (C) Effect of *TAE2* deletion on Hsf1 activity arising from nontranslation stresses.
 See also [Figure S7](#).

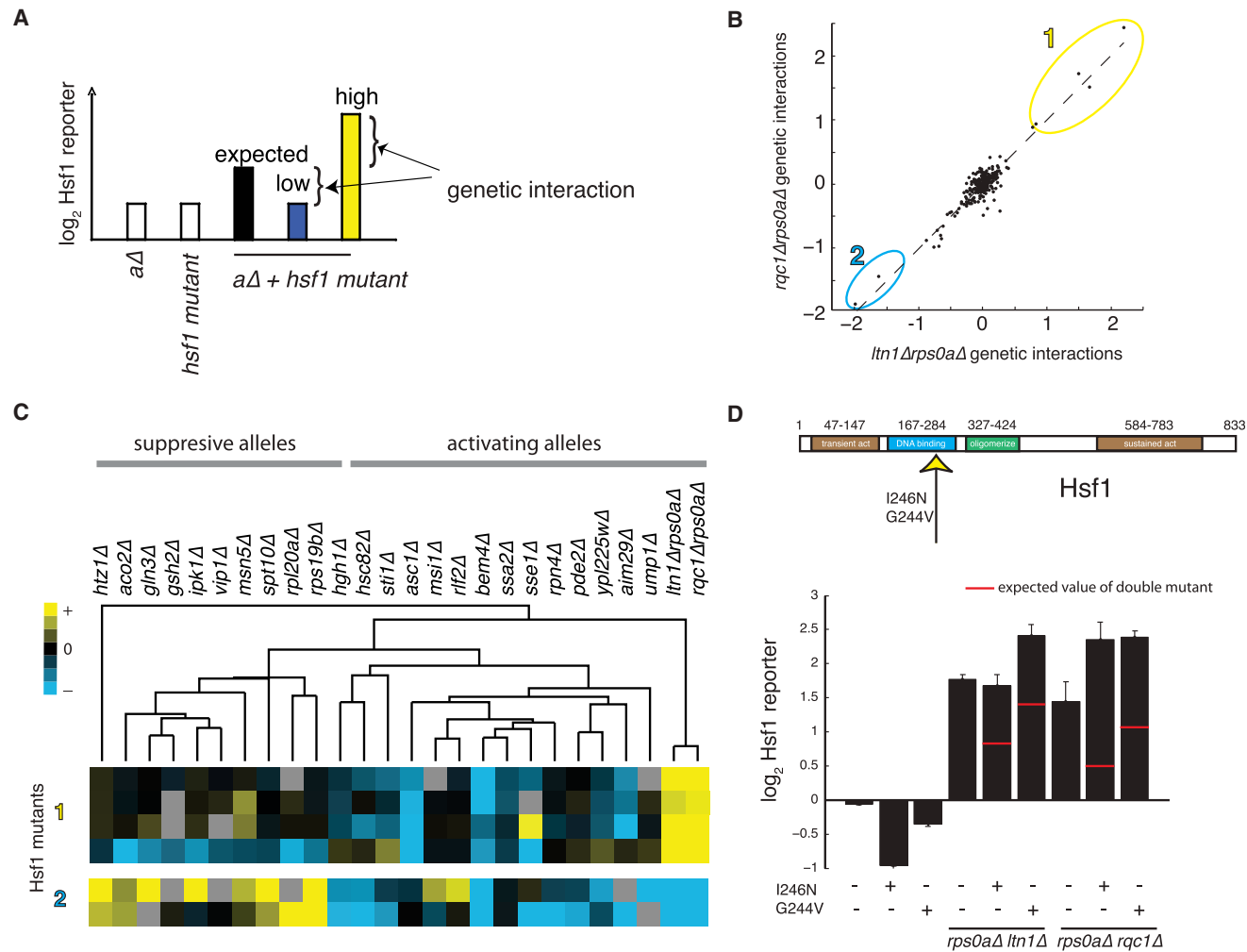


Figure 6. Hsf1 Senses Translation Stress Distinctly from Other Cellular Stresses

(A) Schematic diagram illustrating genetic interactions between loss-of-function alleles and mutant Hsf1 alleles. Procedure is identical to that of Figure 2A, except interactions are computed between *hsf1* mutants and loss-of-function alleles (or pairs of alleles, as are shown in [B]).

(B) Genetic interactions between *hsf1* mutants and double-mutant alleles activating translation-stress signaling. Each point represents one *hsf1* mutant. Strong positive interactors (1) and negative interactors (2) are circled.

(C) Genetic interactions between *hsf1* mutants circled in (B) and loss-of-function alleles having a strong effect on Hsf1 activity. The hierarchical clustering tree shown was calculated from the full set of 290 *hsf1* mutants, not just the six shown.

(D) Hsf1 reporter levels showing genetic interactions between mutations to a region altered in each member of the positive interacting group (I246N and G244V) and genetic backgrounds inducing translation stress. Red marks denote expected values, and deviations from these reveal genetic interactions.

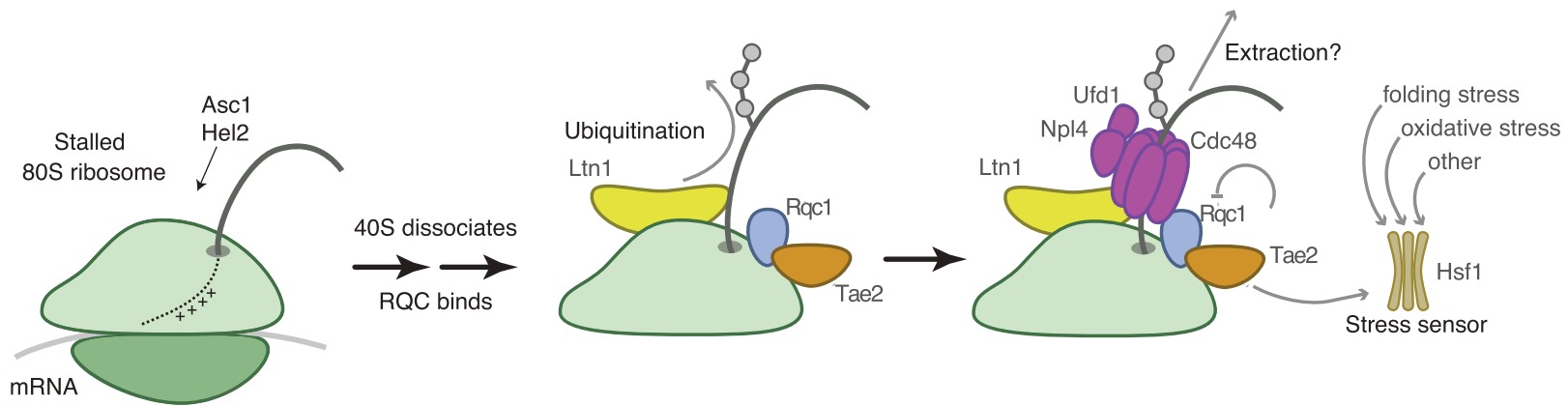


Figure 7. Schematic Model for RQC-Mediated Degradation of Nascent Chains

The 80S ribosome stalls during translation (left). For polybasic substrates (++++ symbol), this is recognized by Asc1 and Hel2 leading to translation termination and possibly RNA cleavage. Ltn1, Rqc1, and Tae2 are then recruited, and the 40S subunit dissociates (the order of these events remains to be determined). Ltn1 then ubiquitylates the nascent chain (second panel), leading to recruitment of Cdc48 and its cofactors Npl4 and Ufd1 (third panel). In addition to its role in substrate ubiquitylation, Tae2 signals translation stress to Hsf1. Levels of Rqc1 are downregulated by the activity of the RQC, leading to a negative feedback loop controlling overall activity of the pathway.

EXPERIMENTAL PROCEDURES

Full descriptions of experiments are included in [Extended Experimental Procedures](#). Briefly, fluorescent Hsf1 and Msn2/4 reporter strains were made from a spore from Y8091, a derivative of S288C (Tong et al., 2001). Hsf1 and Msn2/4 were integrated genomically at the URA3 locus as detailed in [Figure S1](#). By using the synthetic genetic array strategy (Tong et al., 2001), reporter strains were mated to each of ~6,000 strains, each containing a loss-of-function allele. IPs using 3xFLAG epitope strains were grown at 30°C to OD600 1.6 in yeast extract peptone dextrose (YEPD) and then washed in 4°C water before freezing in liquid nitrogen and subsequent mechanical lysis in liquid-nitrogen-cooled conditions. Final elution was done by addition of 3xFLAG peptide. For EM analysis, the immunoprecipitated complex was adsorbed to glow discharged carbon-coated copper grids, stained with uranyl formate, and finally viewed at 42,000× nominal magnification. All fluorescent measurements were performed at 25°C at log phase in synthetic complete media by using a Beckman Dickenson LSR II flow cytometer. Fluorescence values were computed as the median internally normalized values (GFP/RFP for Hsf1 and Msn2/4 reporters; GFP/sidescatter and RFP/sidescatter for polybasic reporter and HSC82pr reporter) for each well. Values were then normalized to WT, and \log_2 scores were computed, so that the WT strain had value 0. All error bars denote SE between duplicate wells on the same multiwell plate or, in the case of western blots, independent experiments. Genetic interaction scores between alleles were computed as the actual double-mutant activity (\log_2 fold basal units) minus the sum of the two single activities (\log_2 fold basal units).

EXTENDED EXPERIMENTAL PROCEDURES

Strains

Fluorescent Hsf1 and Msn2/4 reporter strains were made from a spore from Y8091 (Tong et al., 2001) with MAT α .*his3 Δ 1 leu2 Δ 0 ura3 Δ 0 cyh2 can1 Δ ::STE2pr-spHIS5 lyp1 Δ ::STE3pr-LEU2* background. Hsf1 and Msn2/4 reporters were integrated genomically at the URA3 locus as detailed in Figure S1. Briefly, the HSE reporter strain features a URA3 marked 4xHSE enhancer (Sorger and Pelham, 1987) adjacent to the crippled Cyc1 promoter (Guarente and Ptashne, 1981) driving Emerald GFP (Tsien, 1998) with an actin terminator. 8xSTRE strain was identical but featured repeats of STRE sequence from (Marchler et al., 1993). A *TEF2* promoter driving mKate2 (Shcherbo et al., 2009) with *C. albicans* Adh1 terminator and the URA3 sequence sits directly upstream of the HSE/STRE loci. *HSP82pr* reporter was integrated at the *TRP1* locus. Immunoprecipitations (IPs) in Figures 3A and 3B were performed in the Hsf1 reporter strain with selected target proteins C-terminally tagged with 3xFLAG::Kan cassette (Denic and Weissman, 2007). All other IPs were carried out in BY4741 using a tagged Rqc1 allele. Polybasic reporter measurements were made in BY4741 WT and KanR/NatR (Longtine et al., 1998) single- and double-deletion strains transformed with a derivative of GFP-R12-FLAG-His3 plasmid (Dimitrova et al., 2009), with mKate2 ligated between SpeI and EcoRI. Triple mutants were made using genomic integration of KanR, NatR and HygR (Gritz and Davies, 1983) genes at said loci. The hyperactive *hsf1** allele was made by removing the first 147 amino acids at the endogenous locus, keeping the endogenous promoter. To make the hyperactive *msn2** allele, *MSN2* was amplified from the genome and cloned in front of a constitutive ADH1 promoter, five consensus PKA sites (Görner et al., 1998) were mutated, replacing the phosphorylated serine with alanine. *msn2** was then integrated at the TRP1 locus. Rqc1 FLAG-tagged strains used for Western blotting were made from a BY4741 parent strain. The *ltn1RING Δ* strain was made by truncating endogenous Ltn1 by 57 amino acids. Rqc1 alanine mutant was made in BY4741 by replacing lysines and argenines with alanines (as indicated in Figure 4) using site directed mutagenesis. These mutations and the first 400 nucleotides of the promoter region were inserted using a HIS3 marker at the endogenous locus at the start of the *RQC1* coding region to preserve the promoter of the nearby *SWR1* gene (WT control strain was constructed identically).

Crosses

Using the Synthetic Genetic Array strategy (Tong et al., 2001), the Hsf1, Msn2/4, and polybasic URA-marked reporter strains were mated to each of approximately 6,000 strains each containing a specific loss-of-function allele marked with KanR. Double-mutant strains were created by crossing an Hsf1 reporter strain with NatR-marked loss-of-functional allele (deletion, DAmP, or *hsf1* mutant allele) into KanR-marked loss of function alleles strains, so that the final strains contained both the KanR and NatR marked alleles and the Hsf1 reporter.

SDS-PAGE

All acrylamide gels in this study were NuPAGE Novex 4%–12% Bis-Tris, from Life Technologies, and run in MOPS buffer.

Silver Staining

Silver stains for [Figures 3](#) and [S3](#) were performed using SilverXpress (Life Technologies). [Figures S4](#) and [S5](#) were made using Silver-Quest (Life Technologies).

Western Blotting

Acrylamide gels were transferred to nitrocellulose membranes using the Trans-Blot Sd Semi-Dry Transfer Cell (BIO-RAD) in Nova blot transfer buffer (20% methanol, 2.9% glycine, 5.8% Trizma base, 0.06% SDS). Membrane was blocked at room temperature with Li-Cor Blocking Buffer and then incubated either for 1 hr at room temperature or 4°C overnight at the concentration listed in reagents section below. Membranes were imaged using the Li-Cor Odyssey scanner.

Immunoprecipitations

3xFLAG epitope strains were grown at 30°C to OD1.6 in YEPD and then washed in 4°C water before freezing in liquid nitrogen and subsequent mechanical lysis. Precipitations were then performed in IP buffer containing 50 mM HEPES-KOH pH 6.8, 150 mM KOAc, 5 mM MgOAc, 15% glycerol, 1 mM EDTA, 2 mM DTT, 2x strength complete protease inhibitors (Roche), of 0.1% Igepal CA-630. Lysates were centrifuged twice at 2,800 x G for 10 min and then 300,000 x G for 40 min at 4°C and supernatants were incubated with ANTI-FLAG M2 Affinity Gel (Sigma Aldrich) for 2 hr. After 4x washing in IP buffer, elutions were performed with 3xFLAG peptide (Sigma Aldrich).

RNAase Digestion of IPs

After two spins of raw lysate at 2,800 x G, 5 mM CaCl₂ was and MNASE (micrococcal nuclease) were added to supernatant and incubated for 1 hr at room temperature before addition of 6 mM EGTA to deactivate MNASE. IP was then performed as described above.

Sucrose Gradient of IPs

Sucrose density gradients (10%–50%) were prepared and measured in Seaton Open Top Polyclear centrifuge tubes using a BioComp Gradient Station ip (BioComp Instruments) according to the manufacturer's instructions. Sucrose solutions were prepared

in 20 mM Tris pH 8.0, 140 mM 2KCl, 5 mM MgCl₂, 0.5 mM DTT buffer. Samples were loaded onto gradients, which were spun for 3 hr at 35,000 rpm, 4°C in a SW41 rotor (Beckman Coulter). Samples were finally loaded onto Biocomp Gradient Station ip and the 260 nm absorbance was read using a BIO-RAD Econo UV Monitor.

Negative Stain Electron Microscopy

The immuno-precipitated complex was washed 3x in IP buffer without glycerol or Igepal on Amicon 100 kDa spin columns (Millipore) before being adsorbed to glow discharged carbon-coated copper grids and stained with uranyl formate. Micrographs were collected on an FEI Tecnai12 electron microscope operated at 120kV and 42,000x nominal magnification. Images were collected with a Gatan Ultrascan CCD (final pixel size 2.4 Angstroms). Particles were selected and gray-scale normalized with BOXER as implemented in EMAN ([Ludtke et al., 1999](#)). Contrast Transfer Function (CTF) estimation was performed with CTFFIND3 ([Mindell and Grigorieff, 2003](#)). CTF-correction, two-dimensional classification and averaging were performed via Maximum A Posteriori refinement as implemented in RELION ([Scheres, 2012](#)).

Fluorescence Measurements

Fluorescence was measured using strains grown on multi-well plates using a Becton Dickinson (BD, Franklin Lakes, NJ USA) High Throughput Sampler (HTS). The HTS injected cells directly from the wells they were grown in to a LSRII flow cytometer (BD). All fluorescent measurements were performed at 25°C at log phase in synthetic complete media (SC), except for polybasic reporter in SC-URA media. Matlab 7.8.0 (Mathworks) was then used to compute the median internally-normalized values (GFP/RFP for Hsf1 and Msn2/4 reporters, GFP/sidescatter and RFP/sidescatter for polybasic reporter) for each well. Values were then normalized to WT and log₂ scores computed, so that the wild-type strain had value 0. All error bars are standard error between replicate wells on the same plate. Screening results are based upon a library that may include errors. Any specific allele chosen for follow-up in this study was independently recreated in a fresh strain.

Genetic Interaction Analysis

Interactions between alleles were computed as the actual double-mutant activity (log₂ fold basal units) minus the sum of the two single mutant activities (log₂ fold basal units). Clustering was performed using Cluster 3.0 ([Eisen et al., 1998](#)). Output was viewed with Java Treeview ([Saldanha, 2004](#)).

Mass Spectrometry

Mass spectrometry data were acquired on an AB SCIEX 4800 Plus mass spectrometer.

Reagents

Antibodies: Cdc48 (used at 1:10000) (a gift from Thomas Sommer), mono-ubiquitin (used at 1:10) (P4D1 in serum, a gift of the David Morgan Lab), FLAG (used at 1:5000) (Sigma, F-3165), GFP (used at 1:5000) (Roche, 11814460001), hexokinase (used at 1:10000) (US biologicals, H2035-01), HA used at (1:1000) (Roche, 12CA5), ANTI-FLAG M2 Affinity Gel, (Roche). Cycloheximide was purchased from Sigma-Aldrich (C7698-5G). Error prone PCR for Hsf1 mutagenesis was performed using GeneMorph II Random Mutagenesis Kit with a target error rate of 4-9 errors per kilobase (Agilent Technologies).

Ribosome Profiling

Ribosome profiling was performed in S288C as described in [Ingolia et al. \(2009\)](#) except cells were harvested without addition of cycloheximide. Genes with an average of less than one read per nucleotide were excluded from analysis in [Figure 4A](#).

qPCR

qPCR was performed on a LightCycler 480 (Roche) by performing reverse transcription using oligo-dT primers and then amplifying the cDNA using the following primers: (AATTCCGACCTGAGCAAGAA, CAGTCCAGGCACATGATACG) for *RQC1* and (GTACCCAGCTTCCCAAACA, TTTGTAGCAATGGGACGACA) for *HXK1*.

SUPPLEMENTAL REFERENCES

- Denic, V., and Weissman, J.S. (2007). A molecular caliper mechanism for determining very long-chain fatty acid length. *Cell* 130, 663–677.
- Eisen, M.B., Spellman, P.T., Brown, P.O., and Botstein, D. (1998). Cluster analysis and display of genome-wide expression patterns. *Proc. Natl. Acad. Sci. USA* 95, 14863–14868.
- Gritz, L., and Davies, J. (1983). Plasmid-encoded hygromycin B resistance: the sequence of hygromycin B phosphotransferase gene and its expression in *Escherichia coli* and *Saccharomyces cerevisiae*. *Gene* 25, 179–188.
- Guarente, L., and Ptashne, M. (1981). Fusion of *Escherichia coli* lacZ to the cytochrome c gene of *Saccharomyces cerevisiae*. *Proc. Natl. Acad. Sci. USA* 78, 2199–2203.
- Longtine, M.S., McKenzie, A., III, Demarini, D.J., Shah, N.G., Wach, A., Brachat, A., Philippsen, P., and Pringle, J.R. (1998). Additional modules for versatile and economical PCR-based gene deletion and modification in *Saccharomyces cerevisiae*. *Yeast* 14, 953–961.
- Ludtke, S.J., Baldwin, P.R., and Chiu, W. (1999). EMAN: semiautomated software for high-resolution single-particle reconstructions. *J. Struct. Biol.* 128, 82–97.

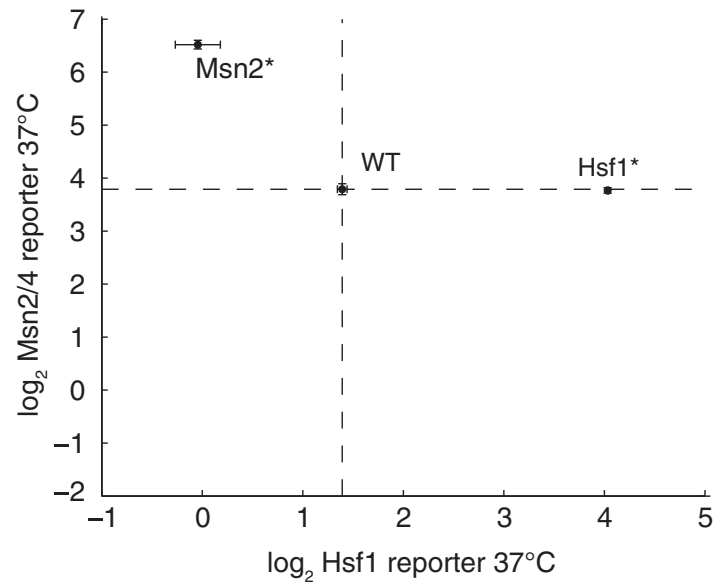


Figure S2. Activation of Msn2/4 Downregulates Hsf1, Related to Figure 1

Activity of Msn2/4 and Hsf1 reporters under wild-type (WT) and constitutively active (*) *msn2* and *hsf1* alleles. Dotted lines mark WT reporter levels.

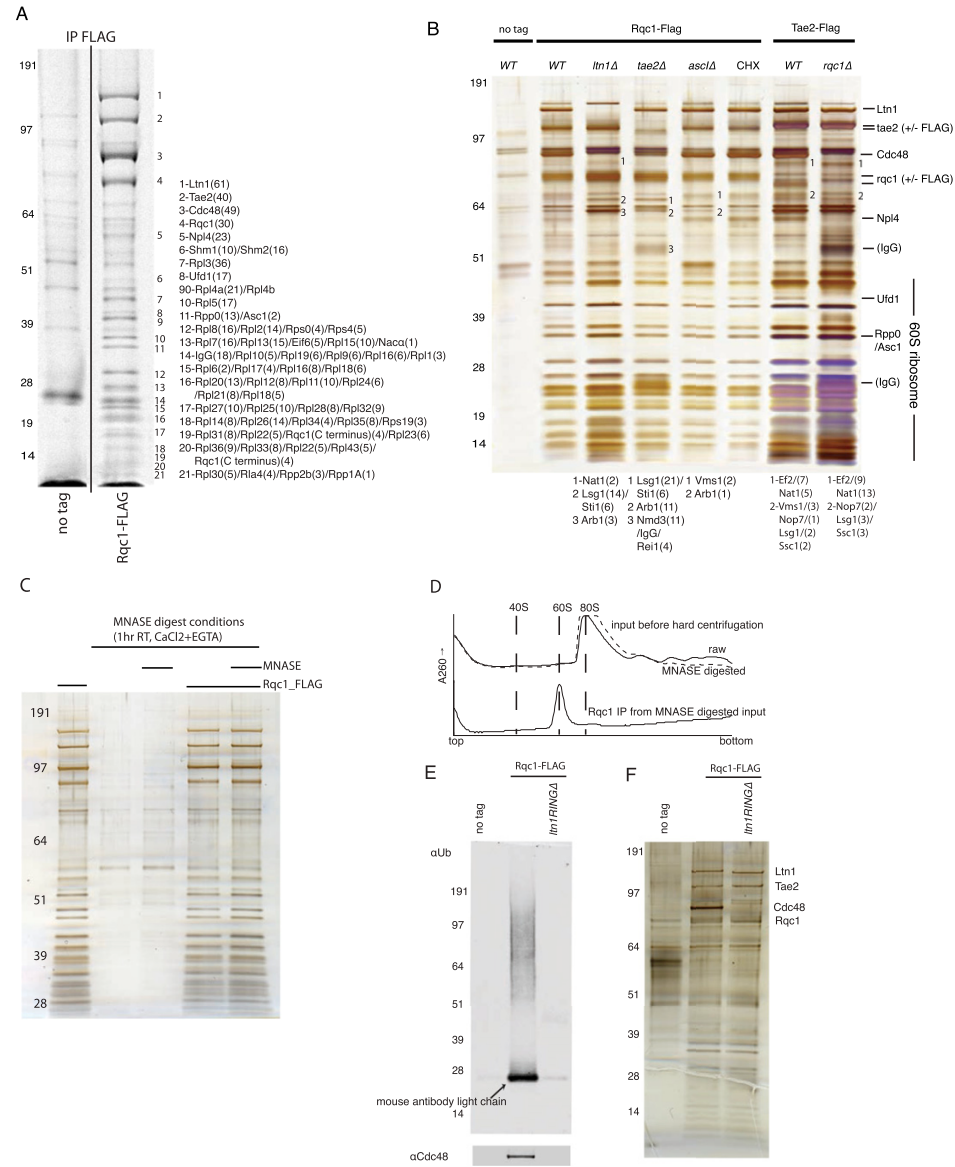


Figure S3. Immunoprecipitation of Rqc1 and Tae2, Related to Figure 3

(A and B) Coomassie (A) and silver-stained (B) IPs in indicated backgrounds with proteins identified by mass spec and not present in control lane labeled. Numbers in parentheses denote the number of unique peptides identified for each protein.

(C) Rqc1 IP under standard conditions and MNAse digestion conditions (described in extended methods).

(D) RNA absorption for 10%–50% sucrose gradient of IP from raw and MNAse digested input before high speed centrifugation step.

(E and F) (E) α Ubiquitin western blot and silver staining (F) of Rqc1-FLAG IP in WT and *ltn1RINGΔ* background.

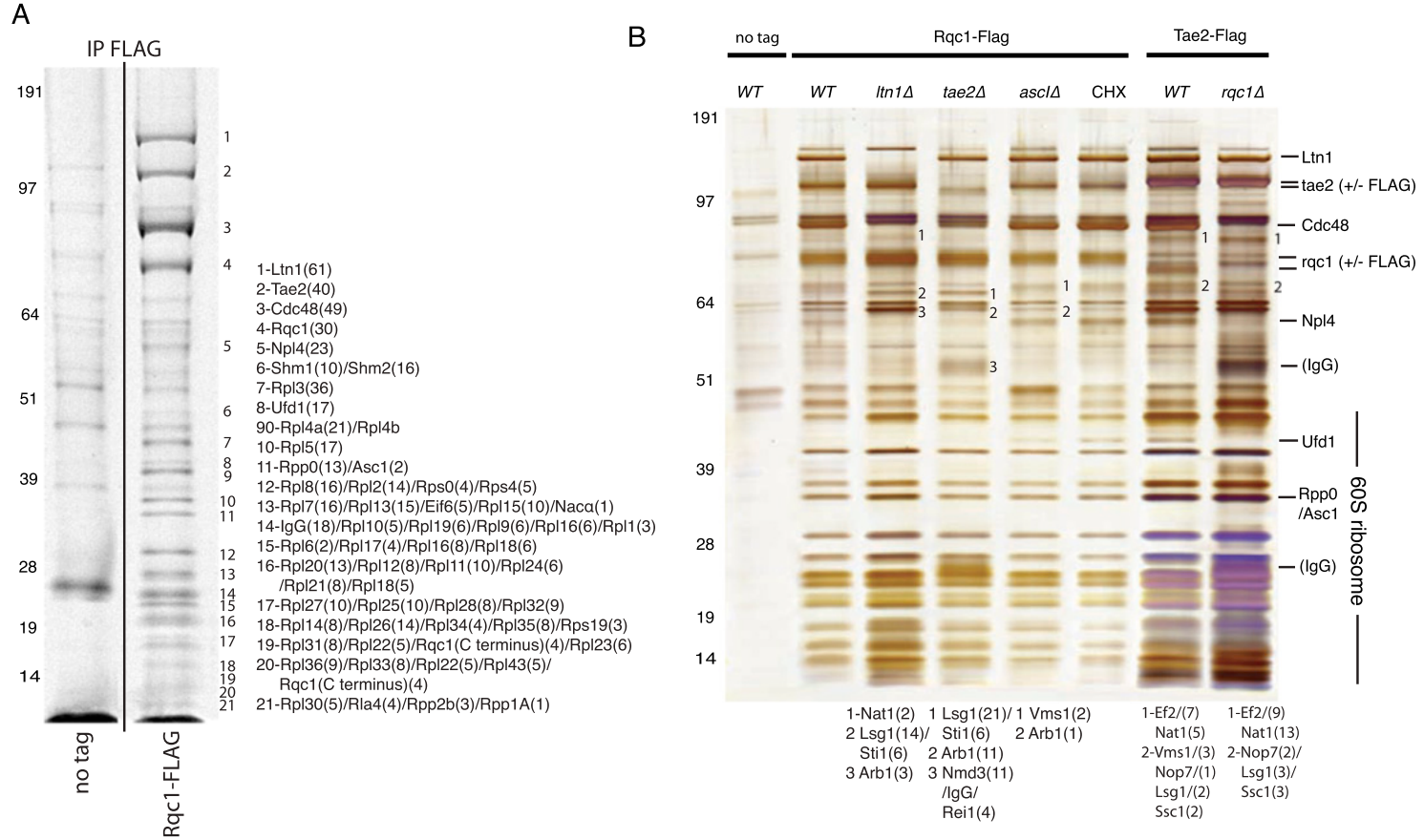


Figure S3. Immunoprecipitation of Rqc1 and Tae2, Related to Figure 3

(A and B) Coomassie (A) and silver-stained (B) IPs in indicated backgrounds with proteins identified by mass spec and not present in control lane labeled. Numbers in parentheses denote the number of unique peptides identified for each protein.

(C) Rqc1 IP under standard conditions and MNASE digestion conditions (described in extended methods).

(D) RNA absorption for 10%–50% sucrose gradient of IP from raw and MNASE digested input before high speed centrifugation step.

(E and F) (E) α Ubiquitin western blot and silver staining (F) of Rqc1-FLAG IP in WT and *ltn1RINGΔ* background.

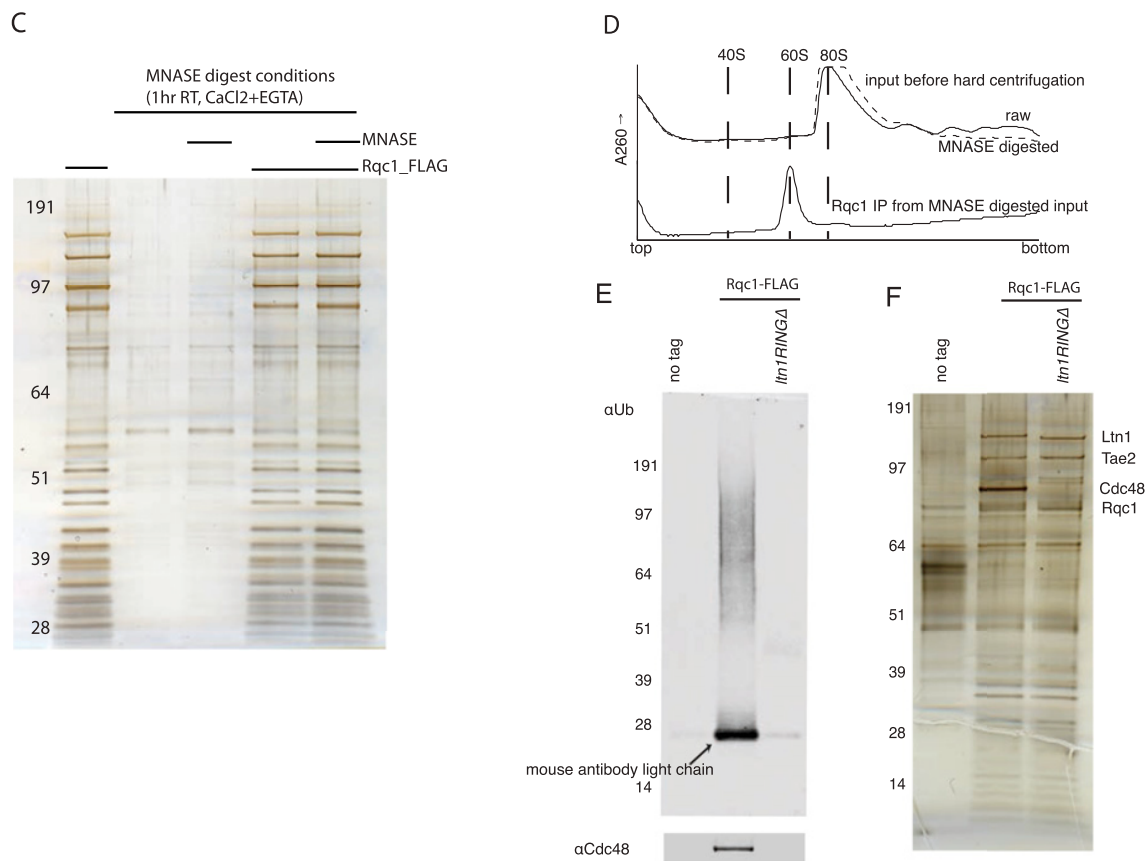


Figure S3. Immunoprecipitation of Rqc1 and Tae2, Related to Figure 3

(A and B) Coomassie (A) and silver-stained (B) IPs in indicated backgrounds with proteins identified by mass spec and not present in control lane labeled. Numbers in parentheses denote the number of unique peptides identified for each protein.

(C) Rqc1 IP under standard conditions and MNASE digestion conditions (described in extended methods).

(D) RNA absorption for 10%–50% sucrose gradient of IP from raw and MNASE digested input before high speed centrifugation step.

(E and F) (E) αUbiquitin western blot and silver staining (F) of Rqc1-FLAG IP in WT and *ltn1RINGΔ* background.

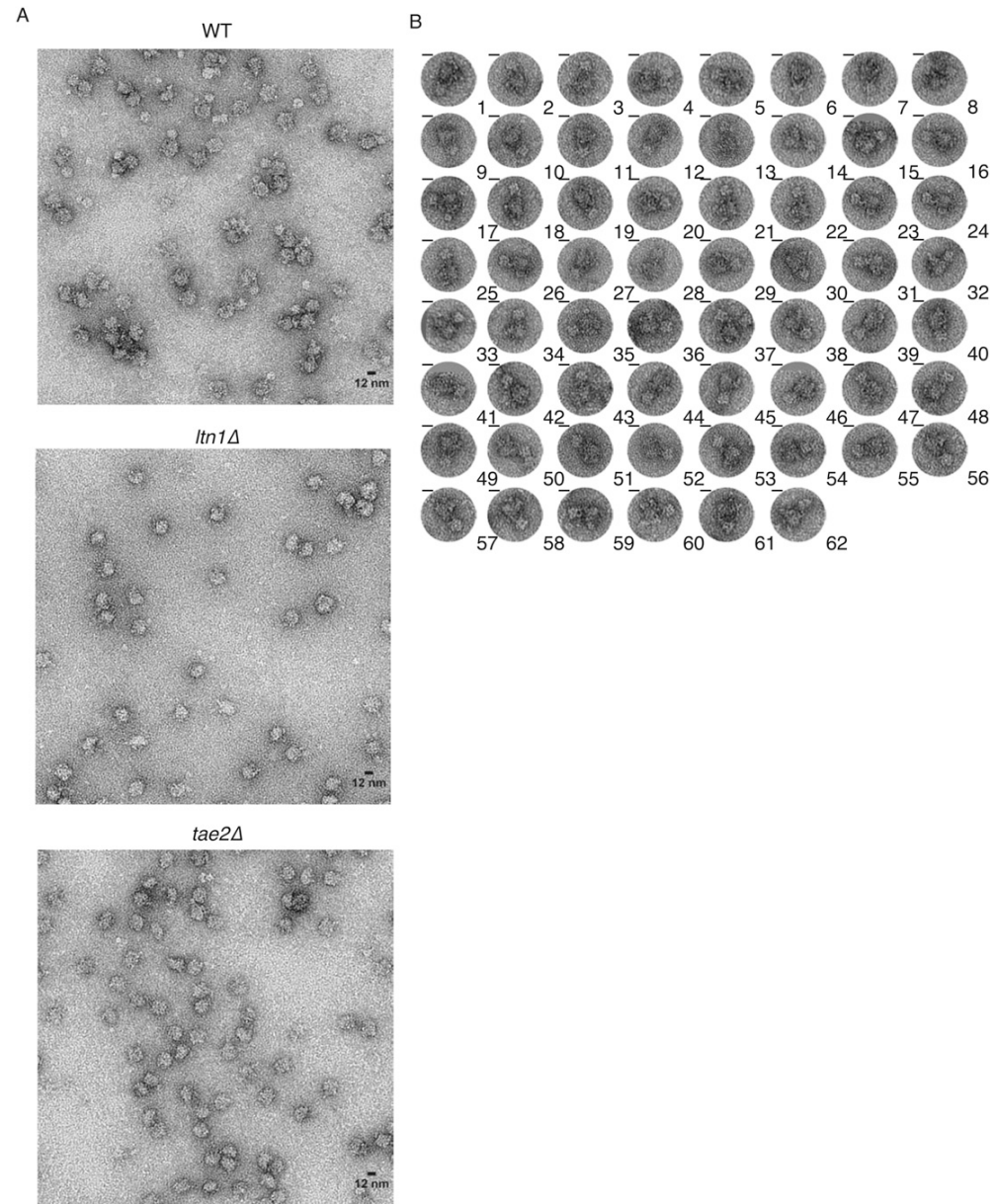


Figure S4. Electron Micrographs of Rqc1 IP, Related to Figure 3

(A) Representative full field micrographs of negative stained Rqc1 immunoprecipitate in wild-type, *ltn1Δ*, and *tae2Δ* backgrounds. (B) 62 raw particles selected from full field micrographs of WT Rqc1 IP. All scale bars are 12 nm.

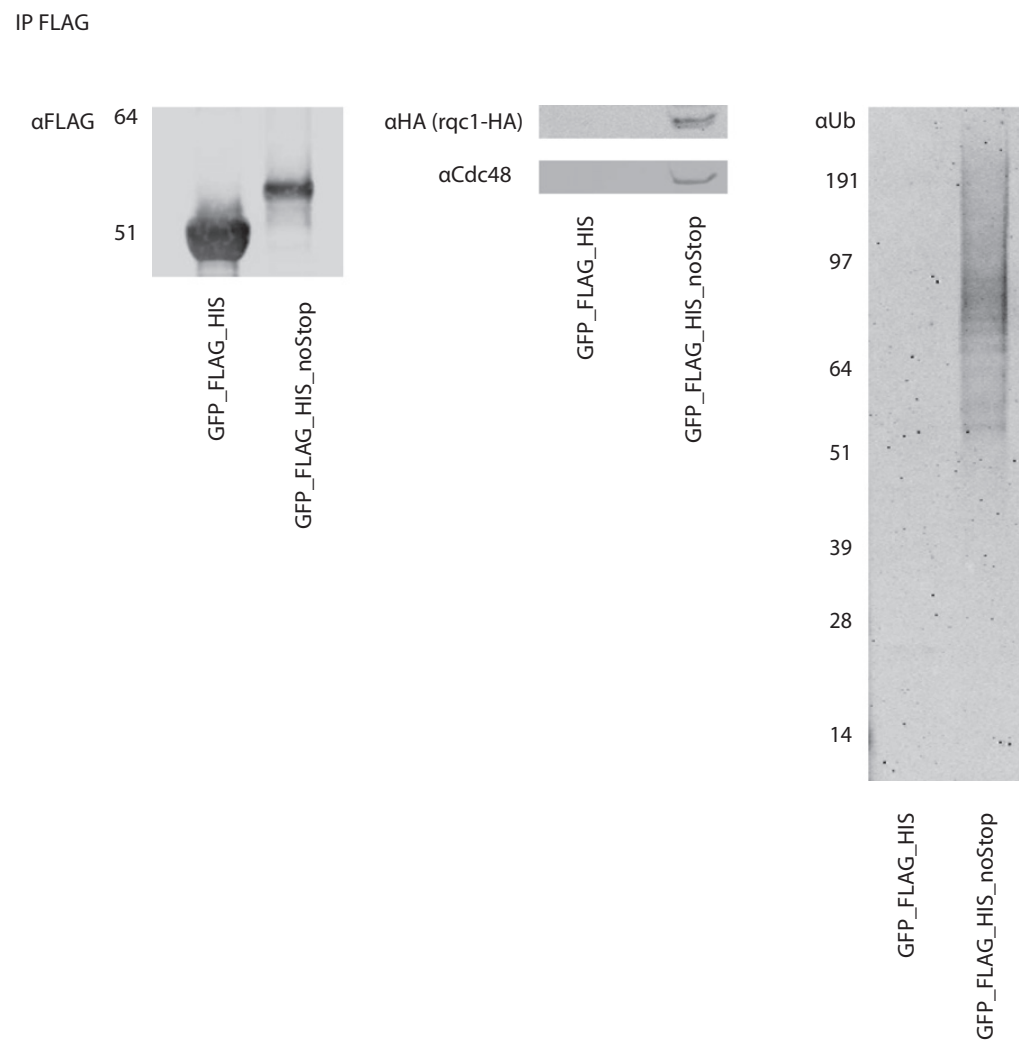


Figure S5. RQC Nonstop Substrate IP in Rqc1-HA Background, Related to Figure 3
 Western blots of GFP_FLAG_HIS(+/-)STOP IP (αFLAG) probing for Ubiquitin, FLAG, Cdc48, an HA (for Rqc1-HA).

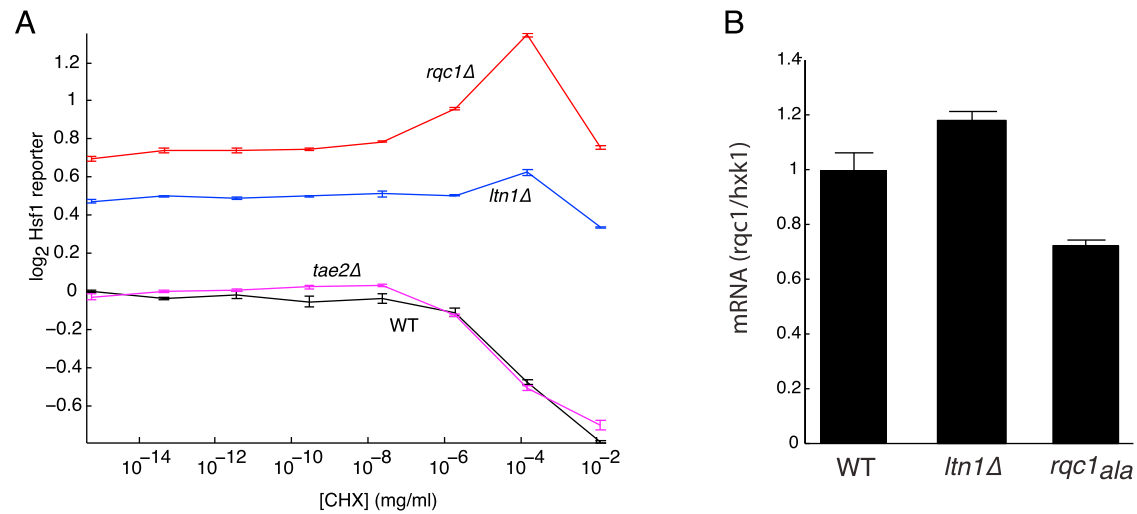


Figure S6. Hsf1 Activity after Cycloheximide and Rqc1 mRNA Levels in RQC Mutants, Related to Figure 4

(A) Hsf1 activity in indicated strains with indicated amount of cycloheximide for 10 hr. Hsf1 activity is normalized by side scatter instead of RFP levels because cycloheximide significantly induces TEF2 activity.

(B) RQC1 mRNA levels in selected backgrounds as measured by qPCR.

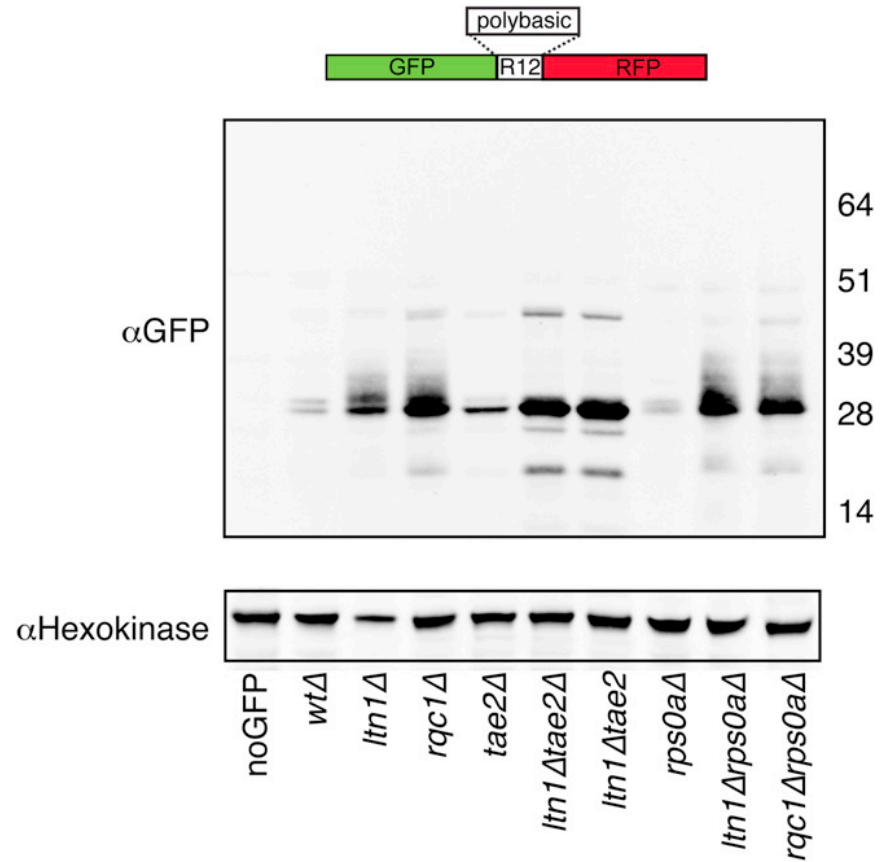


Figure S7. Polybasic Reporter in Selected Deletion Strains, Related to Figure 5
 Western blot probing for GFP in indicated strains expressing polybasic reporter.